Hydrocarbon Seepage Analysis on a Hydrocarbon Field in Indonesia Based on Plant Stress Using Landsat-8 Operational Land Imager and Field Measurements

Tri Muji Susantoro
Faculty of Earth Sciences and Technology, Bandung Institute of Technology

Saepuloh, Asep
Faculty of Earth Sciences and Technology, Bandung Institute of Technology

Wikantika, Ketut
Faculty of Earth Sciences and Technology, Bandung Institute of Technology

Agung Budi Harto
Faculty of Earth Sciences and Technology, Bandung Institute of Technology

他

https://doi.org/10.5109/7183356

出版情報：Evergreen. 11 (2), pp.756-770, 2024-06. 九州大学グリーンテクノロジー研究教育センター
バージョン：

Hydrocarbon Seepage Analysis on a Hydrocarbon Field in Indonesia Based on Plant Stress Using Landsat-8 Operational Land Imager and Field Measurements

Tri Muji Susantoro[1,2*], Asep Saepuloh[1,3*], Ketut Wikantika[1,4], Agung Budi Harto[1,4], Ahmad Maryanto[5]

[1]Faculty of Earth Sciences and Technology, Bandung Institute of Technology, Bandung, 40132, Indonesia
[2]Research Centre for Geoinformatics, Research Organization of Electronics and Informatics, National Research and Innovation Agency, Jakarta, 13710, Indonesia.
[3]Department of Geological Engineering, Bandung Institute of Technology, Bandung, 40132, Indonesia.
[4]Department of Geodesy and Geomatics, Bandung Institute of Technology, Bandung, 40132, Indonesia
[5]Research Centre for Satellite Technology, Aeronautics and Space Research Organization, National Research and Innovation Agency, Jakarta, 13710, Indonesia

*Author to whom correspondence should be addressed:
E-mail: trim010@brin.go.id; saepuloh@itb.ac.id

(Received January 7, 2024; Revised April 15, 2024; Accepted May 13, 2024).

Abstract: Hydrocarbon seepage can impact plants via the root system, which absorbs water and minerals for photosynthesis, and cause plant stress, stunted growth, decreased chlorophyll in the leaf, and plant death. This work aimed to define a vegetation stress pattern on a hydrocarbon field in Indonesia by studying vegetation changes with the Landsat-8 operational land imager (OLI), leaf spectral reflectance and physical plant data. The research was carried out in the West Tugu field, Northwest Java Basin, Indonesia. The six vegetation indices were used to analyze the Landsat-8 OLI and leaf spectral reflectance. The results from Landsat-8 OLI showed the normalized difference vegetation index (NDVI) values in the peripheries areas are 0.2 to 0.3 from 0.2 to 0.73, the green difference vegetation index (GDVI) values in the peripheries areas are 0.06 to 0.13 from 0.06 to 0.39, the enhanced normalized difference vegetation index (ENDVI) values in peripheries areas are 0.21 to 0.37 from 0.21 to 0.64, the leaf area index (LAI) values in peripheries areas are 0.1 to 0.5 from 0.1 to 1.1, and the visible atmospherically resistant index (VARI) values in peripheries areas are -0.2 to -0.11 from -0.13 to 0.16, while the structurally insensitive pigment index (SIPI) values in peripheries areas are 1.5 to 2.0 from 1.0 to 2.0. These results were confirmed by spectral reflectance analysis and the physical plants data from the field survey. Based on the research, we concluded that the most stressed vegetation in the oil and gas field occurred on the peripheries, followed in the middle, and that vegetation outside the peripheries areas was greener and healthier.

Keywords: Landsat-8 OLI; micro-seepage; spectral reflectance; vegetation stress; vegetation Index.

1. Introduction

Hydrocarbon micro-seepage can occur in oil and gas fields, and its distribution can be wider than the reservoir, characterized by mineral alteration[1)]. Hydrocarbon seepage generally consists of gases, primarily methane with a small quantity of ethane and propane[2,3)]. However, seepage can also be in the form of bitumen, evidence of oil accumulation below the surface[4)]. Hydrocarbon seepage can be analyzed geochemically to determine the origin of the oil and gas, and identify potential reservoirs that can store undiscovered hydrocarbon[5)]. Hydrocarbon seepage in the root zone can cause changes in plant pigments, structure, and water content in response to plant stress[6,7)]. Plant stress can be identified using vegetation indices and spectral reflectance properties[7)]. Hydrocarbon seepage, which consists of macro-seepage (visible) and micro-seepage (invisible), generally results from hydrocarbon advection, driven by pressure gradients and permeability along faults, fractures, and bedding planes. Seepage can disrupt soil conditions and contribute to atmospheric emissions[8)].

Hydrocarbon seepage can affect the vegetation in many ways. The root system can absorb the hydrocarbon when it absorbs water and minerals for the photosynthesis process[9)]. Hydrocarbons enter the tissues through

plasmodesmata-mediated slow diffusion from the root surface[10]. Alternatively, hydrocarbon seepage causes a chemically reducing zone in the soil, an increase in the hydrocarbon oxidizing bacteria's activities to degrade n-alkanes[11] and produce carbon dioxide (CO_2) and organic acid, and changes in potential of hydrogen (pH) and oxidation-reduction potential (EH) in the soil[12]. These conditions make the trace elements unstable, dissolved, and displaced[13]. The impact on plants can cause root structure changes and lead to stress, stunted growth, reduced chlorophyll, decreased photosynthetic activities, and plant mortality[9,12–16]. Evidence shows that long-term hydrocarbon seepage causes plants not to grow and forms a circle of bare soil up to 20 m from the source[7]. However, certain plants can grow in soil affected by hydrocarbon contamination[17]. Although the growth of these plants is not good, they are stunted and plant cover becomes sparse[13,18].

Changes in vegetation affect its spectral properties, so that remote sensing methods can detect changes in vegetation even before visual symptoms and negative effects of oil and gas appear[19]. Several remote sensing studies have been conducted to detect the impact of hydrocarbon seepage on plants. This method is one of the most effective methods for tracking the condition of the earth's surface[20]. Hydrocarbon seepage accumulation disrupts the vegetation's health changing the spectral reflectance pattern in remote sensing data. It increases spectral reflectance at visible wavelengths, decreases spectral reflectance at near-infrared wavelengths, and changes the position and shape of the red edge wavelengths[9,18,21,22]. The area affected by the hydrocarbon seepage results in a circle of barren soil around the origin of the seepage, which is surrounded by heavy vegetation[7].

Research in the Niger Delta showed oil pollution in the soil results in biophysical and biochemical alteration of the vegetation and triggers changes in spectral reflectance. These were detected by vegetation indices such as the normalized difference vegetation index (NDVI), soil-adjusted vegetation index (SAVI), adjusted resistant vegetation index (ARVI), green/near-infrared (G/NIR), and green/shortwave infrared (G/SWIR)[23]. Research using Sentinel 2B in north-eastern India shows that NDVI, normalized difference vegetation index red edge (NDVI-RE), Lichtenthaler Index 1 (LIC1), and Simple Ratio Index (SRI) are effective in detecting vegetation stress due to the presence of hydrocarbons on the soil surface, as indicated by the low vegetation index values[24]. Research in the Amazon Forest using hyperspectral images shows that vegetation index analysis (Simple Ratio/SR and NDVI) can distinguish plants experiencing stress due to oil pollution, where the index value is low due to reduced chlorophyll content[14]. Research on pipelines in the provinces of Groningen and Friesland in the Netherlands shows that low NDVI values in vegetation indicate oil and gas pipeline leaks [25].

Indonesia—one of the country that lies on the equator—is characterized by a tropical climate and abundant vegetation. This country has approximately 1,000 hydrocarbon fields, most of which are situated onshore. One of these fields is the West Tugu Barat field (Fig. 1). Micro-seepage is indicated based on the clay mineral anomaly, presented by the apical-halo pattern of the clay mineral total, smectite, and kaolinite[26]. Previous research also found that plants near the West Tugu Field did not grow well[27]. Therefore, detailed research on vegetation changes needs to be carried out; moreover, no studies have been published on vegetation changes and stress patterns in hydrocarbon fields in Indonesia. This study aimed to analyze the vegetation stress pattern in the West Tugu field, Northwest Java Basin, Indonesia, as generated from the spectral reflectance as well as a field survey and Landsat-8 operational land imager (OLI), to prove that the oil and gas reservoir is experiencing micro-seepage, which can disrupt plant growth, that identified based on physical conditions, spectral reflectance, and vegetation indices. This study was carried out to complete the interaction between the presence of oil and gas fields and changes in vegetation above them to understand the biophysical consequences in nature[28]. The result is expected to be applied for hydrocarbon evaluation to improve geological evidence prior to drilling by analyzing prospects for seismic exploration results based on stress vegetation anomalies due to seepage as a manifestation of oil and gas gathering in reservoirs. This research could be the key to oil and gas exploration in Indonesia if it is proven to be successful in distinguishing prospects that are filled with oil and gas from those that are not based on surface micro-seepages. Moreover, the results of a study in the Denver Basin, Colorado, proved that of ten prospects ready to drill, only one contained an anomalous micro-seep found in commercial oil and gas[29].

2. Materials and Methods

The research was conducted in the West Tugu field in Indonesia's West Java Province, located between 6° 31' S and 6° 38' S and 108° 6' E to 108° 14' E (Fig. 1). This area is part of Northwest Java basin, the prolific basin for oil and gas resources in Indonesia[30]. The field is covered with sugarcane plantations, and the crop is grown for approximately 1 year before harvesting[27]. The proven reservoirs for hydrocarbon production include the Upper Cibulakan and Parigi formations, and the source rock is derived from the Talang Akar Formation. The West Tugu field is a hydrocarbon field with an anticline trap type[31].

We employed Landsat-8 OLI, the standard terrain correction Level-1 Terrain (L1T) product, with path/row 121/065. This data can be utilized for spatial variability analysis to characterize the details of the studied area and biomass values [32,33]. The images were captured on September 25, 2015, and downloaded from the United States Geological Survey (https://earthexplorer.usgs.gov/). They were pre-processed with radiometric calibration and atmospheric correction using the fast line-of-sight

atmospheric analysis of hypercubes (FLAASH) method. Radiometric correction is a critical step in processing Landsat-8 OLI to obtain high-quality images[34]. Geometric correction was conducted with reference to the Indonesian topographic map at 1:25,000 scales. The resulting residual mean square error was 0.345.

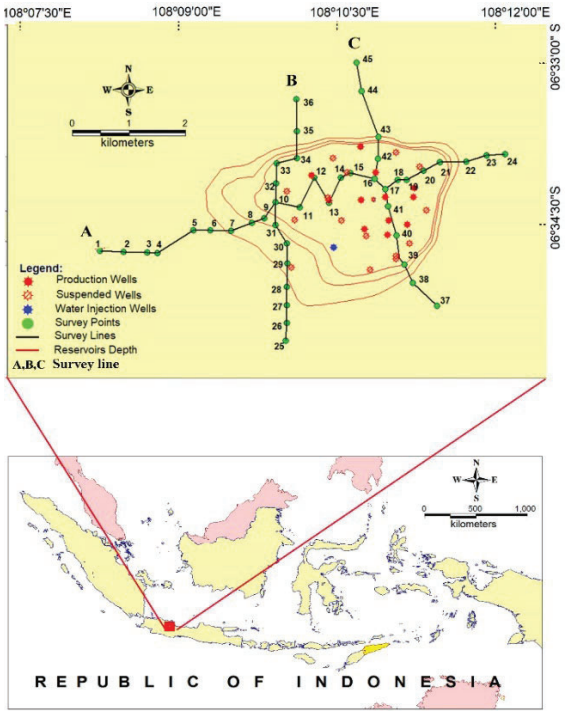

Fig. 1: Research location in the West Tugu field, Northwest Java Basin, Indonesia.

The vegetation index is a remote sensing-based vegetation analysis for quantitative and qualitative evaluation of vegetation cover, vigor, growth dynamics, and other applications[35]. Among the several available vegetation indices, we employed six selected based on the coefficient of determination and standard deviation for 23 vegetation indices[36]. Vegetation indices were utilized to analyze the vegetation stress on the Landsat-8 OLI, and leaf spectral reflectance is in Table 1. The leaf spectral reflectance was also analyzed using red-edge position (REP)[37], and normalized difference vegetation index red-edge (NDVI-RE)[38]. NDVI is an important algorithm for mapping plant distribution by comparing NIR and red bands[39]. Green difference vegetation index (GDVI) is a vegetation index that maps nitrogen in plants[40]. Enhanced normalized difference vegetation index (ENDVI) is a development of NDVI to represent the existence and condition of green vegetation and highlight aspects of vegetation density[41]. Leaf area index (LAI) is a vegetation index that estimates leaf cover, plant growth, and crop yields[42]. Structurally insensitive pigment index (SIPI) monitors plant health, detects plant stress, determines seasonal crop production, and performs crop yield analysis[43]. Visible atmospherically resistant index (VARI) estimates vegetation fractions with low sensitivity to atmospheric effects[44]. Red-edge position (REP) is an index used to estimate the wavelength of the red edge position, which is sensitive to changes in chlorophyll concentration [37,45]. NDVI-RE is a vegetation index used for precision agricultural mapping, forest monitoring, and vegetation stress detection[38]. The results are expected to provide an overview of the vegetation stress pattern on the hydrocarbon ground surface, especially in the West Tugu field, Northwest Java Basin, Indonesia.

The first field survey was conducted in March 2017 using three survey lines that crossed the hydrocarbon field with 45 sample points (Fig. 1). The time of the survey was the end of the rainy season, so the soil, which is dominated by clay, is expected to become saturated and trap gas[48]. Another important consideration is that the sugarcane plant is in the third phase, or rapid growth phase[27,49]. Measurements of physical data (sugarcane height, clump, and segment number) and leaf spectral reflectance were determined at each sample point (Fig. 2). This measurement step was repeated three times at each sample point, and the average value was used as representative data for vegetation stress analysis. Spectral reflectance was measured on the leaf with optimal growth, characterized by a dark green color. The tool is a hyperspectral Field-Spec analytical spectral device (ASD) at wavelengths of 350–2500 nm. The second field survey was conducted in August 2017 to observe sugarcane growth around the hydrocarbon field. The challenges faced during the survey were damaged road conditions and social insecurity due to land ownership conflicts between residents and sugar companies in the study location. Therefore, two local workers were used to make the survey more manageable and avoid social conflicts with residents.

Statistical analysis was conducted between the physical characteristics of sugarcane and vegetation indices from the Landsat-8 OLI and leaf spectral reflectance. This calculation uses linear regression and the coefficient of determination (R^2). These results were then used to identify whether the vegetation indices were related to the physical characteristics of sugarcane or whether the change in the leaf's internal structure resulted from micro-seepage on the ground surfaces. Although an indirect relationship may be found between the physical characteristics of sugarcane and leaf internal structure changes, both might have been equally affected by micro-seepage.

The vegetation stress pattern was analyzed descriptively to depict changes in vegetation characteristics due to the presence of micro-seepage on/or near the surface. This condition is indicated as a manifestation of hydrocarbons in the reservoir. This research was based on vegetation analysis using visual and physical field observations, vegetation index analysis using spectral reflectance, and Landsat-8 OLI.

Table 1. Band ratios for vegetation analysis.

Vegetation Indices	Algorithms
NDVI (normalized difference vegetation index)[46]	$\frac{(NIR - Red)}{(NIR + Red)}$
GDVI (green difference vegetation index)[47]	$NIR - Green$
ENDVI (enhanced normalized difference vegetation index)[41]	$\frac{((NIR + Red) - (2 \times Blue))}{((NIR + Green) + (2 \times Blue))}$
LAI (leaf area index)[42]	$3.618 + \left(2.5 \times \left(\frac{(NIR - Red)}{(NIR + (6 \times Red) - (7.5 \times Blue) + 1)}\right) - 0.118\right)$
SIPI (structurally insensitive pigment index)[43]	$\frac{(NIR - Blue)}{(NIR - Red)}$
VARI (visible atmospherically resistant index)[44]	$\frac{(Green - Red)}{(Green + Red - Blue)}$
REP (red-edge position)[37]	$700 + 40 \times \left(\frac{\left(\left(\frac{(R_{670} + R_{780})}{2}\right) - R_{700}\right)}{(R_{740} - R_{700})}\right)$
NDVI-RE (normalized difference vegetation index-red edge)[38]	$\frac{(R_{750} - REP)}{(R_{750} + REP)}$

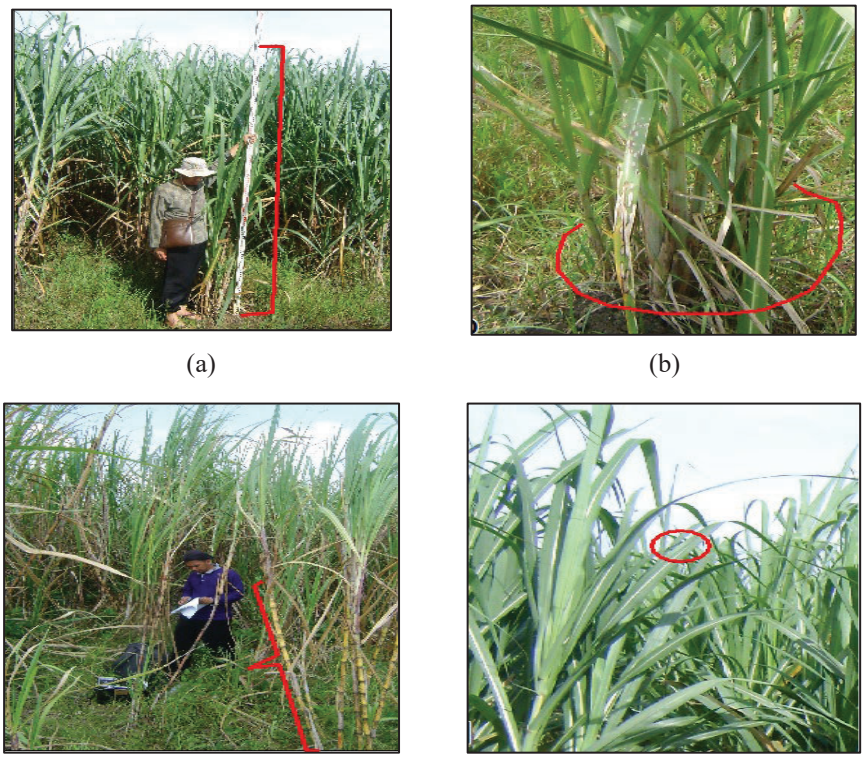

(a) (b) (c) (d)

Fig. 2: Field measurements (red outline indicates the measurement target), including (a) sugarcane height, (b) sugarcane clump, (c) sugarcane segment, and (d) upper leaf surface measured with ASD hyperspectral instrument.

Potential hydrocarbon seepage is identified based on an analysis of the physical condition of vegetation, Landsat-8 OLI data vegetation index, and spectral reflectance. The steps taken include: (1) describing the results of physical observations of vegetation spatially in three cross sections. (2) identify the physical condition of the vegetation at each point and analyze the anomalies that occur. (3) The results of the vegetation index from Landsat-8 OLI data and spectral reflectance were also sampled at the same location as physical field observations with 3 cross sections to identify the vegetation anomalies on the oil and gas fields. (4) Overlay with oil and gas field data conducted to analyze the pattern of vegetation stress. (5) Based on the anomaly pattern, a descriptive model of oil and gas field anomalies was created, supported by existing concepts from previous research. The challenge in this research is that Landsat-8 OLI data has a spatial resolution of 30m x 30m, even though the survey was carried out based on sampling points per plant clump. However, the uniform condition of the sugarcane plants per plot with an area of around 250 m x 250 m means that the sampling results can be considered representative of that plot.

3. Result and Discussion

3.1. Physical characteristics of vegetation

The physical characteristics of sugarcane resulting from the field survey are illustrated in Fig 3. The height ranged from 1.2 m to 4.1 m, with an average value of 2.8 m and a standard deviation of 0.8. Further, the number of clumps ranged from 2 to 27 trees with an average value of 11 and a standard deviation of 4.9, and the number of segments ranged from 2 to 19 with an average value of 10 and a standard deviation of 5.3. The taller sugarcane tended to occupy the field's northwestern and outer section areas, while the shorter sugarcane grew in a circular pattern from the southern to northeastern peripheries. Generally, the sugarcane in the middle tended to be taller than that on the southern peripheries but shorter than that the northwestern peripheries.

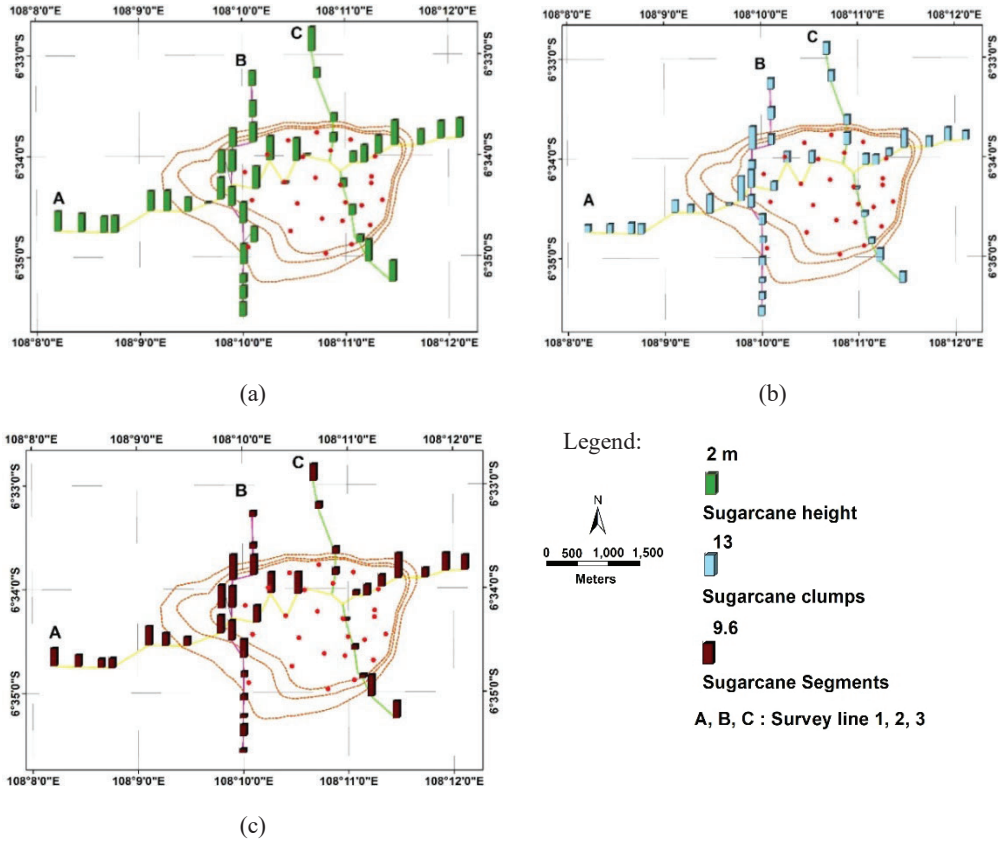

Fig 3: Graphs showing the physical characteristics of sugarcane; (a) sugarcane height, (b) sugarcane clumps, and (c) sugarcane segments.

The densest clumps were observed in the northwestern area, whereas the least dense clumps grew circularly from the south to the northeastern peripheries. Overall, the sugarcane clumps in the middle were denser than those on the peripheries but less dense than those in the northwestern area of the field. The highest sugarcane segment distribution was observed in the northwestern area of the field, and the lowest was observed from the south to the eastern peripheries. Sugarcane exhibited stunted growth with a low density on the peripheries, as depicted by points 11, 18, 29, 33, 40, and 43 in Fig. 4. In August, five months after the field survey, sugarcane on the southern peripheries was yellowish, dry, or not harvestable, indicating the existence of micro-seepage,

that confirmed in the survey results, where: (1) survey line A, the average tree height in the active oil and gas well area is 1.6 m, while outside the active oil and gas well is 2.9 m; (2) survey line B, which is located outside active oil and gas wells, has an average sugarcane tree height of 2.8 m; and (3) survey line C, the average height of sugarcane trees around active oil and gas wells is 1.0 m and outside active oil and gas wells is 2.6 m (Fig. 3). The survey results also found gas seeps, and oil seeps around hydrocarbon wells (Fig. 4). Gas seepage is characterized by the presence of gas bubbles in the water, while oil seepage appears black and thick. In locations where seepage occurs, the condition of the vegetation does not grow well.

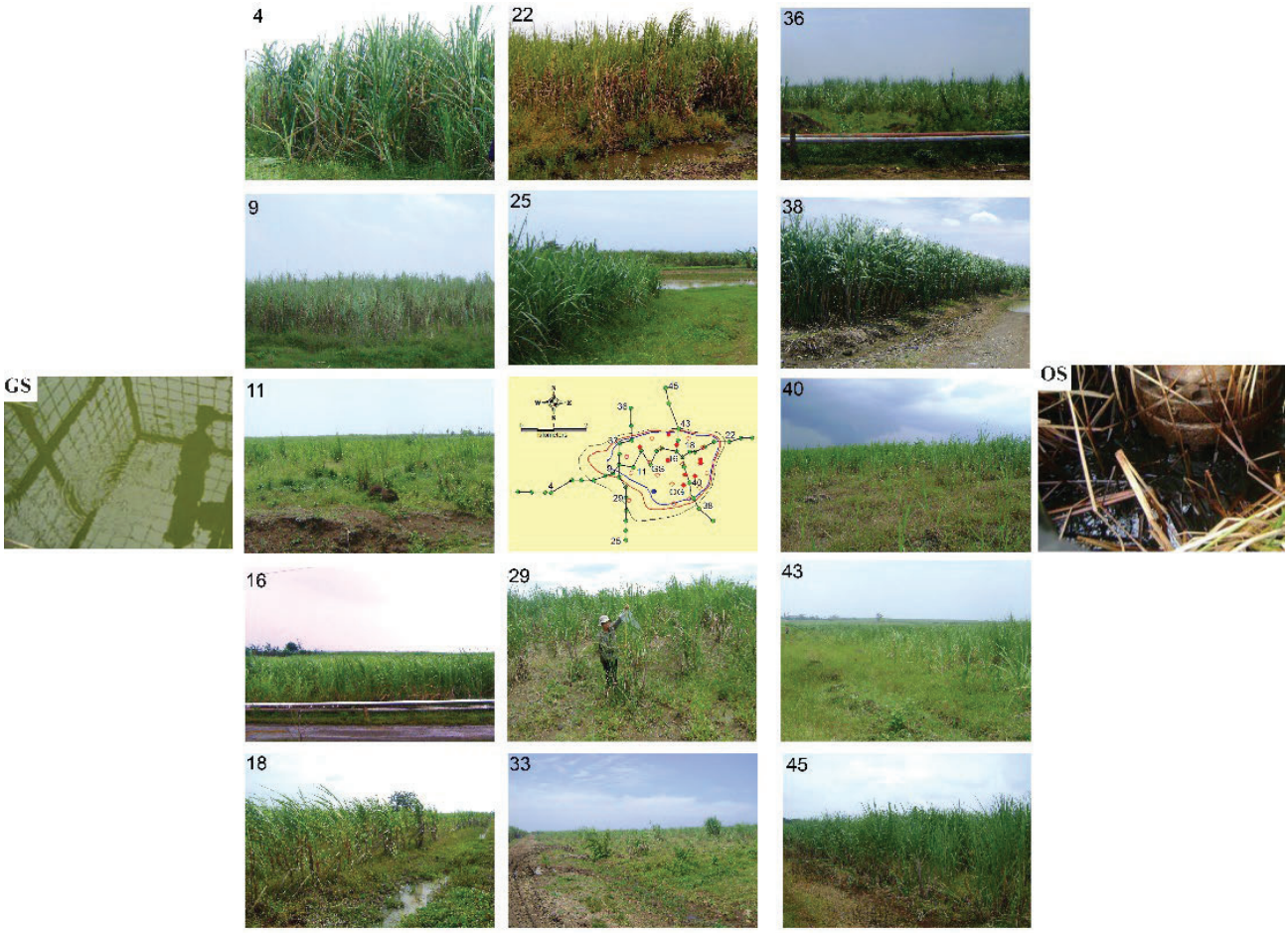

Fig. 4: Images of sugarcane around the hydrocarbon field showing stunted plant growth with low density on the peripheries.

3.2 Vegetation anomaly mapping

The results showed that the index values in NDVI, GDVI, ENDVI, LAI, and VARI on Landsat-8 OLI revealed the same patterns, which are higher in the outside- peripheries area and lower in the peripheries area (Figs. 5 and 6). The detailed vegetation index values are as follows: (1) The NDVI values of vegetation areas are 0.2 to 0.73, with the values in the peripheries areas being 0.2 to 0.3; (2) the GDVI values of vegetation areas are 0.06 to 0.39, with the values in the peripheries areas being 0.06 to 0.13; (3) the ENDVI values of vegetation areas are 0.21 to 0.64, with the values of peripheries areas being 0.21 to 0.37; (4) the LAI values of vegetation areas are 0.1 to 1.1, with the values of peripheries areas being 0.1 to 0.5; and (5) the VARI values of vegetation areas are -0.32 to 0.16, with the values of peripheries areas being -0.2 to -0.11. These results conform to the physical characteristics of sugarcane discussed above. Based on the detailed pattern, the vegetation index values in the middle area were higher than those on the peripheries but lower than those in the outside- peripheries area. In contrast, the structurally insensitive pigment index (SIPI) value was high on the peripheries (Fig. 5e and Fig. 7b). The high SIPI indicated high carotenoid content that led to a decline in vegetation health. Hence, these indices serve as indicators of vegetation stress[43].

The VARI values were lower and more uniform than those of the other vegetation indices due to the use of the visible wavelength for analysis. Where the low spectral reflectance values of the visible wavelength caused a lower band ratio between those channels than that found for the other vegetation indices (Fig. 5f and Fig. 7f). This result differed from those observed for the near-infrared

(NIR) band ratio and red channels[44]. The results derived from the detailed observation of vegetation indices on Landsat-8 OLI at 45 sample points on the three survey lines are illustrated in Figs. 6 and 7. Overall, high values for NDVI, GDVI, ENDVI, LAI, and VARI were found on the outside- peripheries area, while low values were found on the south to the eastern peripheries, forming a circular pattern (Figs. 6b–6f).

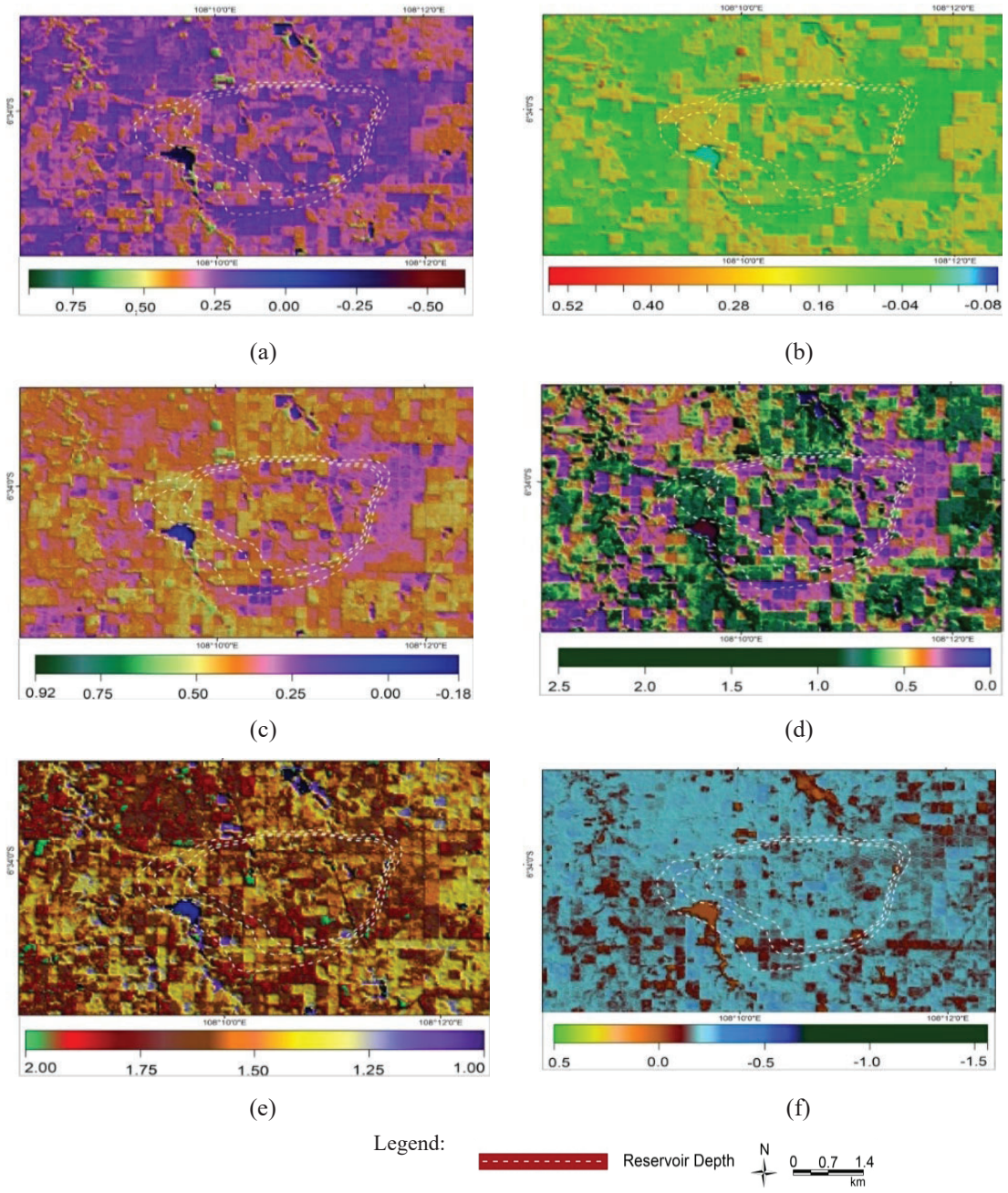

Fig. 5: Map of the vegetation indices around West Tugu field obtained from the Landsat-8 OLI; (a) NDVI, (b) GDVI, (c) ENDVI, (d) LAI, (e) SIPI, and (f) VARI.

The different values of SIPI on Landsat-8 OLI were unclear; however, high values tended to occupy the peripheries areas (Fig. 7a). The values of SIPI for vegetation areas are 1.0 to 2.0, and the values for peripheries areas are 1.5 to 2.0. While SIPI values on leaf spectral reflectance recorded by ASD were very clear; high values tended to occupy the middle – near peripheries area (Fig. 7b). The dominant low values for the vegetation indices tended to occupy the middle to near peripheries areas, forming a circular "halo" pattern. This pattern indicated intensive of micro-seepage.

The results of the spectral reflectance of leaves, which was recorded using ASD, are illustrated in Fig. 6a. The leaf spectral reflectance readouts at sample points 11, 12, 38, and 39 were high in the NIR region, aligning with the research reported in the previous[50]. Parallel to the

reflectance pattern, survey line 1 showed that the leaf spectral reflectance at visible wavelengths increased from the middle to the eastern peripheries area of the field. Further, survey line 2 showed that the leaf spectral reflectance at visible wavelengths increased from the south to the eastern peripheries area of the field, and survey line 3 showed that the leaf spectral reflectance at visible wavelengths increased from the middle to the southern peripheries of the field.

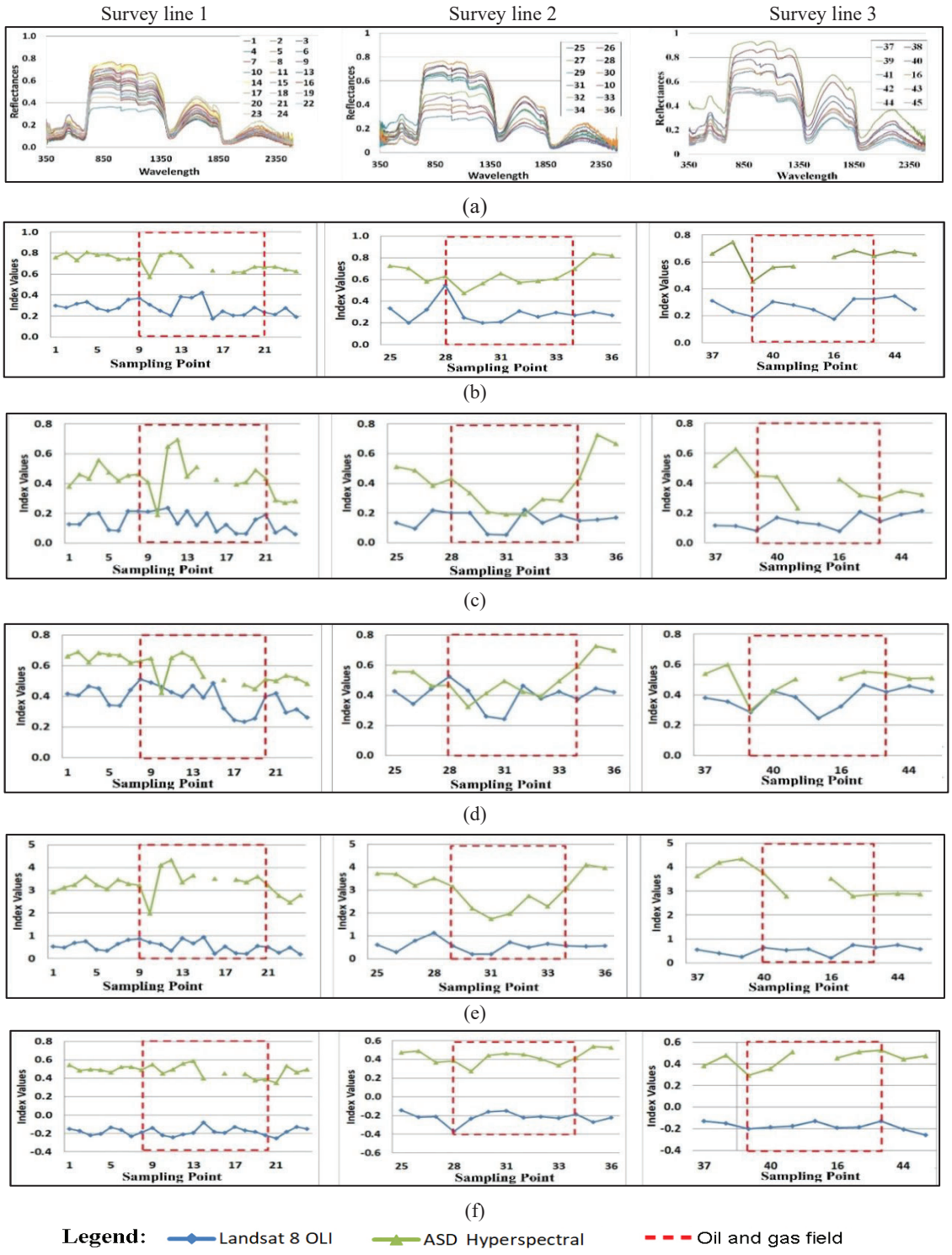

Fig. 6: Leaf spectral reflectance recorded by ASD in the three survey lines and vegetation index results in the survey lines on leaf spectral reflectance and Landsat-8 OLI. (a) spectral reflectance readouts, (b) NDVI, (c) GDVI, (d) ENDVI, (e) LAI, and (f) VARI. Survey lines have been depicted by Fig. 1

We performed an additional analysis using REP and NDVI-RE on the leaf spectral reflectance resulting from ASD. Those analyses were conducted to confirm that vegetation stress existed as an impact of micro-seepage. The REP results ranged from 705 to 722 nm, with an average value of 717 nm (Fig. 7c). In survey line 1, the REP changes showed the same pattern as the vegetation index on leaf spectral reflectance. The REP shifted to a shorter wavelength at leaf spectral reflectance in the middle hydrocarbon and peripheries areas. However, the REP still had higher wavelength values in the middle area than those obtained in the peripheries areas. This condition was also observed in survey lines 2 and 3. Our results confirmed the previous research, revealing that the changes in leaf spectral reflectance due to natural gases led to a REP shift toward shorter wavelengths [9,50]. The NDVI-RE also had the same pattern as the REP and other vegetation indices on leaf spectral reflectance (Fig. 7d). These findings confirmed that the sugarcane experienced different levels of stress, with more stress on the peripheries and the middle areas than those on the outside-peripheries area, indicating that micro-seepage influenced the sugarcane in the hydrocarbon field.

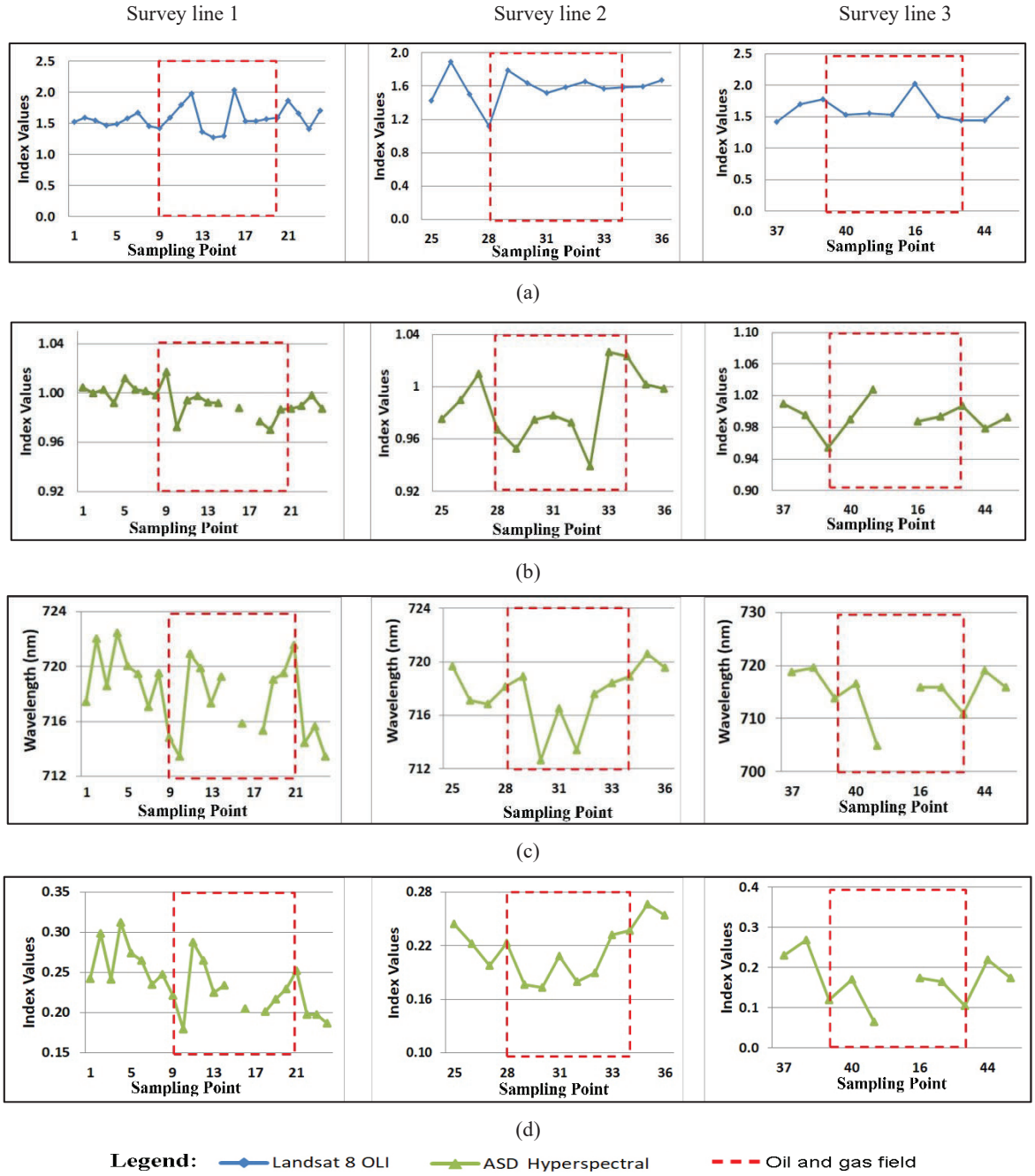

Fig. 7: Vegetation index results in the survey lines on leaf spectral reflectance and Landsat-8 OLI. (a) SIPI on Landsat-8 OLI, (b) SIPI on leaf spectral reflectance, (c) REP, and (d) NDVI-RE. Survey lines have been depicted by Fig. 1.

3.3 Correlation between physical characteristics of plant and vegetation indices

The highest correlation among the physical characteristics of sugarcane was found between sugarcane height and the number of segments, with an R^2 of 0.687. The correlation between sugarcane height and clumps had an R^2 of 0.196. The correlation between the physical characteristics of sugarcane and vegetation indices was generally low. The highest correlation was found between sugarcane height and NDVI-RE, $R^2 = 0.244$ (Table 2). The correlation of the physical characteristics of sugarcane and vegetation indices was lower in the Landsat-8 OLI than in the leaf spectral reflectance (Table 2). Due to the spectral reflectance on the Landsat-8 OLI was produced not only from the pure leaf spectral reflectance but also from the combination of objects existing in the 1-pixel size.

Table 2. Values for the coefficient of determination (R^2) between the physical characteristics of sugarcane and vegetation indices.

Data	Vegetation Index	The physical characteristics of sugarcane		
		Height (R^2)	Clump (R^2)	Segment (R^2)
Landsat-8 OLI	ENDVI	0.003	0.072	0.008
	GDVI	0.003	0.108	0.001
	NDVI	0.000	0.020	0.032
	LAI	0.000	0.064	0.016
	SIPI	0.020	0.002	0.031
	VARI	0.005	0.191	0.030
Spectral Reflectance from ASD	ENDVI	0.043	0.023	0.003
	GDVI	0.012	0.016	0.022
	NDVI	0.079	0.028	0.009
	LAI	0.012	0.019	0.125
	SIPI	0.001	0.038	0.008
	VARI	0.005	0.091	0.000
	REP	0.137	0.006	0.025
	NDVI-RE	0.244	0.046	0.077

Based on the coefficient of determination, we estimated that the leaf spectral reflectance is generally more influenced by the internal structure and leaf pigment. The impact of physical characteristics of trees such as height, number of clumps, or segments on spectral reflectance tends to be low. These results align with previous research, where the hydrocarbon can cause chlorophyll degradation, water content, and leaf structure[6,9,14,51]. Hydrocarbons can affect vegetation through the root system by absorbing water and minerals for photosynthesis[9]. Hydrocarbons also affect vegetation by binding to soil chemical elements that cause hydrocarbon-oxidizing bacteria to increase and produce more CO_2 and organic acids, resulting in changes in pH and oxidation-reduction potential in the soil[12]. Besides that, several oil and gas fields are sources of CO_2[52].This condition causes the plant root structure system to change, and the vegetation experiences stress, stunted growth, reduced chlorophyll in leaves, and plant death[9,12,13,15].

3.4 Impact of hydrocarbon seepage

The leaf spectral reflectance of the sample points in Fig. 6a indicated different values in the visible wavelength and the shortwave infrared regions. This result indicated that the effect of micro-seepage could be analyzed based on the sugarcane leaf spectral reflectance in the visible wavelength area, which had higher values in the middle area than in the outside-peripheries areas. The results align with previous research, revealing that micro-seepage leads to increased values of leaf spectral reflectance in the visible wavelength area and decreased values in the NIR area [9].

The analysis of vegetation indices on Landsat-8 OLI (Figs. 6b–6f and 7a) and the leaf spectral reflectance (Figs. 6b–6f and 7b–7c) indicated a consistent change in the sugarcane conditions in the hydrocarbon field, characterized by altered index values. Vegetation indices were generated by comparing the spectral reflectance of the visible and NIR wavelengths. These wavelengths are sensitive to changes in vegetation conditions, including biochemical and biophysical characteristics caused by micro-seepage[50]. The REP and NDVI-RE (Fig. 7c–7d) analyses also confirmed the results for NDVI, GDVI, ENDVI, LAI, SIPI, and VARI; the results were more sensitive in detecting changes in vegetation stress because the REP information can be used to monitor the vegetation stress conditions[53]. The indication of vegetation stress is revealed at the REP, which shifts toward shorter wavelengths with the decrease in the level of leaf chlorophyll due to micro-seepage[9]. Additionally, NDVI-RE had the same index values as the other vegetation indices, indicating that NDVI-RE was highly responsive to even the slightest changes in the ratio of chlorophyll a and b; hence, it is useful for the early detection of vegetation stress[53].

The analysis of vegetation indices on the Landsat-8 OLI and leaf spectral reflectance revealed that the lowest value was found in the peripheries areas of the hydrocarbon field,

indicating a high zone of micro-seepage around the peripheries areas of the field. This condition aligns with previous research, where in the seepage zone, plant growth is stunted, and further away from oil and gas fields, the plants grow well[13,21,54,55]. Zuhui et al.'s research confirms that vapor migration occurs intensively at the edge of the field and then forms gas seepage velocity near the surface[56]. In addition, at the edge of the field, there is also the enrichment of radon, illite, uranium, thoron, delta carbon, gypsum, cobalt, chromium, nickel, lead, arsenic, zinc, copper, vanadium, molybdenum, thallium, gallium, and magnetic minerals[57].

3.5 Vegetation stress pattern

Spatial analysis of the vegetation index on Landsat-8 OLI showed that the change in sugarcane spectral reflectance was indicated as the impact of the presence of micro-seepage (Fig. 5). The low values for the vegetation indices affirmed plant stress conditions characterized by stunted growth and low-density. This condition aligns with the sampling plot of the vegetation indices on Landsat-8 OLI, which provided an overview of the effect of micro-seepage on sugarcane (Figs. 6 and Fig. 7). Further, the results of the vegetation indices on the leaf spectral reflectance and physical characteristics of sugarcane (Fig 3, Fig. 4, and Fig. 5) strengthened the analysis results from the Landsat-8 OLI on the vegetation indices regarding the presence of micro-seepage. A combination of Landsat-8 OLI and leaf spectral reflectance recorded with ASD was useful for assessing the vegetation stress pattern.

Based on the analysis of the vegetation indices and physical characteristics of sugarcane, micro-seepage was concluded to have occurred on the field surface; this was identified based on low vegetation index values, low plant density, and stunted plant growth in the south and eastern areas. Additionally, the changes in clay minerals that occurred in the surface soil of the hydrocarbon field may have indicated the presence of micro-seepage[26]. Previous research pointed out that the presence of hydrocarbon seepage results in stunted plant growth and decreased density[58]. The stress condition was also verified by the high leaf spectral reflectance in the visible region obtained from ASD measurements. This finding was consistent with the previous research on vegetation stress due to the impacts of hydrocarbon seepage[13,21,25].

The vegetation stress pattern on the hydrocarbon field based on the vegetation indices from the Landsat-8 OLI, leaf spectral reflectance, and physical characteristics of sugarcane revealed that the most stressed vegetation occurred on the peripheries areas, indicating the presence of intensive micro-seepage (Fig. 8). This result is consistent with the distribution of radon emissions near the oil and gas field surface, which tends to be higher at the edge of the field[59]. Previous research confirmed that vegetation stress was dominant at the peripheries of the field[13,21]. In these areas, the hydrocarbon diffusion process migrates vertically[12,54], the chimney column extends from the middle to peripheries areas to enable migration of the hydrocarbon to the surface[13], and the fracture increases at the structural margin owing to the rock compactness difference[57], vapor gas migration[56], hydrocarbon content enrichment, mineralization, paraffin dirt, waxes, salt metals, and microbes[57]. The vegetation is still affected in the middle areas, where the micro-seepage migrates vertically to the likely impermeable areas through diffusion processes[54,60] or the chimney column[13,60]. This chimney column causes hydrocarbons to migrate within a relatively short time[61].

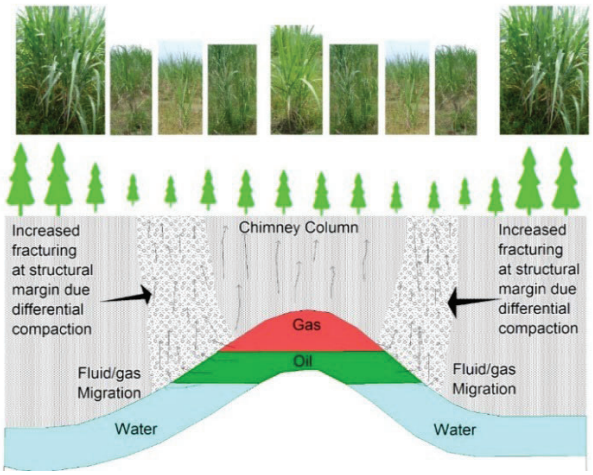

Fig. 8: Vegetation stress pattern in the West Tugu field based on the vegetation index, spectral reflectance, and physical characteristics.

This research can be employed to confirm the presence of hydrocarbons in onshore drillable prospects in hydrocarbon basins in Indonesia. Before drilling an exploration well, a surface anomaly study should be carried out to identify the presence of micro-seepage as an indication of the presence of oil and gas in the reservoirs. Observations of the expression of oil and gas structures that sometimes appear on the surface also need to be carried out to support the study of surface anomalies[62]. The positive anomaly shown by the vegetation stress around the hydrocarbon field could provide concrete evidence for increasing the success of drilling. The advantage of surface anomalies for detecting hydrocarbon seepage is also suggested to be conducted to enhance the success ratio of exploration drilling[61]. Based on a review of more than 1100 wildcat wells, more than 80% of the wells resulted in positive commercial discoveries based on the anomaly, and only 11% of wells were drilled without the association of such anomalies that resulted in hydrocarbon discoveries. Other researchers also confirmed that the success ratio of prospects with a micro-seepage anomaly was nearly 82% of the hydrocarbon discoveries[63].

The results of this research can also be used for environmental monitoring. The existence of vegetation anomalies proves that in oil and gas fields, seepage can

occur, which has the potential to cause emissions and increase global warming[55]. Hydrocarbon seep is also one of the sources of greenhouse gases in the form of methane and propane gas enrichment in the environment[64]. Research in America shows that the upstream oil and gas industry is a source of of enrichment of methane and propane gas in the environment[65]. Around 25% of oil and gas accumulation in reservoirs is estimated to be lost slowly over a long geological time[66].

4. Conclusion

Based on the analysis of the Landsat-8 OLI, leaf spectral reflectance, and physical characteristics of sugarcane on the hydrocarbon field, we conclude that the stressed vegetation was identified as the impact of micro-seepage on the ground surface. Micro-seepage originates from reservoirs migrating to ground surfaces. The pattern exhibited that the most stressed vegetation occurred in the peripheries areas, followed by the middle areas. This pattern indicates that micro-seepage was more intense in the peripheries areas than in the middle areas. This evidence can also be seen physically based on the condition of plants experiencing stress and stunting at the edge of the field, which is also confirmed by various vegetation indices that show low index values at the edge of the field. In future research, a comprehensive analysis should be conducted via measurement and analysis of the amount of hydrocarbon in soil and enrichment of oil biodegradation bacteria. This comprehensive research will provide more definitive evidence for the presence of micro-seepage on the ground surface.

Acknowledgements

We thank the RIIM/LPDP organization, the Dean, and the Staff of the Faculty of Earth Sciences and Technology, Bandung Institute of Technology for facilitating this research to completion. We also thank the staff and leaders of the Research Centre for Remote Sensing–Research Organization for Aeronautics and Space–National Research and Innovation Agency for supporting this research. We thank Mrs. Fitria Agustin and the laboratory staff at the Geological Survey Center, Geological Agency, for allowing us to use the ASD hyperspectral instrument; Yudhi, Hari, and Triwijaya for their assistance with the field survey; the Chairman and Researcher Staff at the Group of Exploration Technology Research Program-LEMIGAS-Ministry of Energy and Mineral Resources who helped prepare the survey equipment and laboratory instruments for sample analysis during the study; and all individuals who assisted with this research.

Nomenclature

OLI	operational land imager
NDVI	indices normalized difference vegetation index
GDVI	green difference vegetation index
ENDVI	enhanced normalized difference vegetation index
LAI	leaf area index
VARI	visible atmospherically resistant index
REP	red-edge position
NDVI-RE	NDVI red-edge
EH	oxidation-reduction potential
SAVI	soil-adjusted vegetation index
ARVI	adjusted resistant vegetation
G	green
NIR	near Infrared
SWIR	Shortwave infrared
FLAASH	fast line-of-sight atmospheric analysis of hypercubes
SIPI	structurally insensitive pigment index
ASD	analytical spectral device
R^2	the coefficient of determination
R_{750}	Reflectance 750 nm (band 750 nm)
nm	nanometer
m	meter

References

1) S. Chen, Y. Zhao, L. Zhao, Y. Liu, and C. Zhou, ‘Hydrocarbon micro-seepage detection by altered minerals mapping from airborne hyper-spectral data in xifeng oilfield, china’, *Journal of Earth Science*, 28 (*4*) 656–665 (2017). doi:10.1007/s12583-015-0604-1.
2) J.R. Boles, G. Garven, and C. Peltonen, ‘Hydrocarbon production reduces natural methane seeps in the santa barbara channel’, *Marine and Petroleum Geology*, 151 (*December 2022*) 106187 (2023). doi:10.1016/j.marpetgeo.2023.106187.
3) A. Boruah, S. Verma, A. Rasheed, G. Siddharth Gairola, and A. Gogoi, ‘Macro-seepage based potential new hydrocarbon prospects in assam-arakan basin, india’, *Scientific Reports*, 12 (*1*) 2273 (2022). doi:10.1038/s41598-022-06045-6.
4) R. Schinteie, A.S. Ross, C.J. Boreham, R.H. Kempton, A. Talukder, and C. Trefry, ‘Petroleum source rocks in the bight basin, australia: an updated view’, *Marine and Petroleum Geology*, 151 (*January*) 106165 (2023). doi:10.1016/j.marpetgeo.2023.106165.
5) A.J. Al-Khafaji, A. Alattabi, S. Y. Jassim, and F. Sadooni, ‘Oil-polluted groundwater in central and west iraq as indicator of potential new hydrocarbon plays’, *Petroleum Science and Technology*, 1–19 (2023). doi:10.1080/10916466.2023.2209122.
6) G. Lassalle, A. Credoz, R. Hédacq, S. Fabre, D. Dubucq, and A. Elger, ‘Assessing soil contamination due to oil and gas production using vegetation hyperspectral reflectance’, *Environmental Science & Technology*, 52 (*4*) 1756–1764 (2018). doi:10.1021/acs.est.7b04618.
7) M.F. Noomen, H.M.A. van der Werff, and F. van der

Meer, 'Spectral and spatial indicators of botanical changes caused by long-term hydrocarbon seepage', *Ecological Informatics*, 8 55–64 (2012). doi:10.1016/j.ecoinf.2012.01.001.
8) G. Etiope, 'A global dataset of onshore gas and oil seeps: A new tool for hydrocarbon exploration', 2009. http://www.earth-prints.org/handle/2122/6040.
9) K.L. Smith, M.D. Steven, and J.J. Colls, 'Spectral responses of pot-grown plants to displacement of soil oxygen', *International Journal of Remote Sensing*, 25 (*00*) 1–17 (2004). doi:10.1080/01431160410001729172.
10) M. Alkio, T.M. Tabuchi, X. Wang, and A. Colón-Carmona, 'Stress responses to polycyclic aromatic hydrocarbons in arabidopsis include growth inhibition and hypersensitive response-like symptoms', *Journal of Experimental Botany*, 56 (*421*) 2983–2994 (2005). doi:10.1093/jxb/eri295.
11) R. Narmanova, A. Tapalova, R. Zhapparbergenov, and N. Appazov, 'Biological products for soil and water purification from oil and petroleum products', *Evergreen*, 10 (*2*) 688–695 (2023). doi:10.5109/6792815.
12) F. Van Der Meer, P. Van Dijk, H.M.A. van der Werff, and Y. Hong, 'Remote sensing and petroleum seepage: a review and case study', *Terra Nova*, 14 (*1*) 1–17 (2002). doi:10.1046/j.1365-3121.2002.00390.x.
13) D. Schumacher, 'Hydrocarbon-induced alteration of soils and sediments', in: D. Schumacher, A.M. A (Eds.), AAPG Memoir, The American Association of Petroleum Geologists, 1996: pp. 71–89. doi:10.1306/m66606c6.
14) P. Arellano, K. Tansey, H. Balzter, and D.S. Boyd, 'Detecting the effects of hydrocarbon pollution in the amazon forest using hyperspectral satellite images', *Environmental Pollution*, 205 225–239 (2015). doi:10.1016/j.envpol.2015.05.041.
15) Y. Naudé, M.W. van Rooyen, and E.R. Rohwer, 'Evidence for a geochemical origin of the mysterious circles in the pro-namib desert', *Journal of Arid Environments*, 75 (*5*) 446–456 (2011). doi:10.1016/j.jaridenv.2010.12.018.
16) M.F. Noomen, A.K. Skidmore, F.D. van der Meer, and H.H.T. Prins, 'Continuum removed band depth analysis for detecting the effects of natural gas, methane and ethane on maize reflectance', *Remote Sensing of Environment*, 105 (*3*) 262–270 (2006). doi:10.1016/j.rse.2006.07.009.
17) M. Abdullah, Z. Al-Ali, A. Abulibdeh, M. Mohan, S. Srinivasan, and T. Al-Awadhi, 'Investigating the succession process of native desert plants over hydrocarbon-contaminated soils using remote sensing techniques', *Environmental Research*, 219 (*December 2022*) 114955 (2023). doi:10.1016/j.envres.2022.114955.
18) M.F. Noomen, 'Hyperspectral reflectance of vegetation affected by underground hydrocarbon gas seepage', 2007. http://www.itc.nl/library/papers_2007/phd/noomen.pdf.
19) A. Gholizadeh, and V. Kopačková, 'Detecting vegetation stress as a soil contamination proxy_ a review of optical proximal and remote sensing techniques', *International Journal of Environmental Science and Technology*, 16 (*5*) 2511–2524 (2019). doi:10.1007/s13762-019-02310-w.
20) A. Yussupov, and R.Z. Suleimenova, 'Use of remote sensing data for environmental monitoring of desertification', *Evergreen*, 10 (*1*) 300–307 (2023). doi:10.5109/6781080.
21) Y. Hong, 'Imaging spectrometry for hydrocarbon microseepage', International Institute for Geo-Information Science and Earth Observation, 1999.
22) M.I. Jamaludin, A.N. Matori, and K.C. Myint, 'Application of NIR to determine effects of hydrocarbon microseepage in oil palm vegetation stress', in: 2015 International Conference on Space Science and Communication (IconSpace), IEEE, Langkawi, Malaysia, 2015: pp. 215–220. doi:10.1109/IconSpace.2015.7283791.
23) B. Adamu, K. Tansey, and B. Ogutu, 'Using vegetation spectral indices to detect oil pollution in the niger delta', *Remote Sensing Letters*, 6 (*2*) 145–154 (2015). doi:10.1080/2150704X.2015.1015656.
24) R. Kashyap, 'Vegetation stress as chief indicator for detection of hydrocarbon microseepage in regions of north-eastern india', *Spatial Information Research*, 571–584 (2022). doi:10.1007/s41324-022-00453-6.
25) H.M.A. van der Werff, M. van der Meidje, F. Jansma, F. van der Meer, G.J.J. Groothuis, M. der Meijde, F. Jansma, F. der Meer, G.J.J. Groothuis, M. van der Meidje, F. Jansma, F. van der Meer, G.J.J. Groothuis, M. der Meijde, F. Jansma, F. der Meer, G.J.J. Groothuis, M. van der Meidje, F. Jansma, F. van der Meer, and G.J.J. Groothuis, 'A spatial-spectral approach for visualization of vegetation stress resulting from pipeline leakage', *Sensors*, 8 (*6*) 3733–3743 (2008). doi:10.3390/s8063733.
26) T.M. Susantoro, A. Saepuloh, F. Agustin, K. Wikantika, and A.H. Harsolumakso, 'Clay mineral alteration in oil and gas fields: integrated analyses of surface expression, soil spectra, and x-ray diffraction data', *Canadian Journal of Remote Sensing*, 46 (*2*) 237–251 (2020). doi:10.1080/07038992.2020.1771174.
27) T.M. Susantoro, K. Wikantika, A.B.B. Harto, and D. Suwardi, 'Monitoring sugarcane growth phases based on satellite image analysis (a case study in indramayu and its surrounding, west java, indonesia)', *HAYATI Journal of Biosciences*, 26 (*3*) 117–128 (2019). doi:10.4308/hjb.26.3.117.
28) B.K. Yermekbayev, N. V. Dzhangarasheva, and G.M. Rakhimzhanova, 'Overview of grazing as a land use system in kazakhstan', *Evergreen*, 10 (*2*) 658–666 (2023). doi:10.5109/6792812.
29) D. Schumacher, 'Minimizing Exploration Risk: The

Impact of Hydrocarbon Microseepage Surveys for Distinguishing Hydrocarbon-Charged Traps from Traps Without Hydrocarbons', in: AAPG Annual Meeting, AAPG, Houston, Texas. USA, 2017: pp. 1–9.

30) B. Muljana, K. Watanabe, and M.F. Rosana, 'Source-rock potential of the middle to late miocene turbidite in majalengka sub-basin, west java indonesia: related to magmatism and tectonism', *Journal of Novel Carbon Resources Sciences*, 6 15–23 (2012). https://qir.kyushu-u.ac.jp/dspace/handle/2324/25218.
31) B. Puspoputro, and E. Lubis, 'The geophysical case history of Rengasdengklok area, North West Java', in: 21st Annual Convention Proceedings Indonesian Petroleum Association, The AAPG/Datapages Combined Publications Database, Jakarta, Indonesia, 1992: pp. 1:361-378. https://archives.datapages.com/data/ipa/data/021/021001/361_ipa021a0361.htm.
32) S. Singh, S.K. Singh, R. Kumar, A. Shrama, and S. Kanga, 'Finding alternative to river sand in building construction', *Evergreen*, 9 (*4*) 973–992 (2022). doi:10.5109/6625713.
33) B. Pranoto, I. Adilla, H. Soekarno, N. Konitat Supriatna, L. Efiyanti, D. Anggraini Indrawan, N. Widya Hesty, and S. Rahmah Fithri, 'Using satellite data of palm oil area for potential utilization in calculating palm oil trunk waste as cofiring fuel biomass', *EVERGREEN Joint Journal of Novel Carbon Resource Sciences & Green Asia Strategy*, 10 (*3*) 1784–1791 (2023). doi:10.5109/7151728.
34) H. Kausarian, Lady Redyafry, J.T.S. Sumantyo, A. Suryadi, and M.Z. Lubis, 'Structural analysis of the central sumatra basin using geological mapping and landsat 8 oli/tirs c2 l1 data', *Evergreen*, 10 (*2*) 792–804 (2023). doi:10.5109/6792830.
35) J. Xue, and B. Su, 'Significant remote sensing vegetation indices: a review of developments and applications', *Journal of Sensors*, 2017 1–17 (2017). doi:10.1155/2017/1353691.
36) T.M. Susantoro, K. Wikantika, A. Saepuloh, and A.H. Harsolumakso, 'Selection of vegetation indices for mapping the sugarcane condition around the oil and gas field of north west java basin, indonesia', *{IOP} Conference Series: Earth and Environmental Science*, 149 (*1*) 12001 (2018). doi:10.1088/1755-1315/149/1/012001.
37) J.G.P.W. Clevers, S.M. De Jong, G.F. Epema, F. van der Meer, W.H. Bakker, A.K. Skidmore, and K.H. Scholte, 'Derivation of the red edge index using the meris standard band setting', *International Journal of Remote Sensing*, 23 (*16*) 3169–3184 (2002). doi:10.1080/01431160110104647.
38) A.A. Gitelson, and M.N. Merzlyak, 'Spectral reflectance changes associated with autumn senescence of aesculus hippocastanum l. and acer platanoides l. leaves', *Journal Plant Physiology*, 143 (*3*) 286–292 (1994). doi:10.1016/S0176-1617(11)81633-0.
39) S.T. Brantley, J.C. Zinnert, and D.R. Young, 'Application of hyperspectral vegetation indices to detect variations in high leaf area index temperate shrub thicket canopies', *Remote Sensing of Environment*, 115 (*2*) 514–523 (2011). doi:10.1016/j.rse.2010.09.020.
40) R.. Sripada, R.. Heinigerb, G. Whitec, J, and A.. Meijer, 'Aerial color infrared photography for determining early in-season nitrogen requirements in corn', *Agronomy Journal*, 98 (2006).
41) Maxmax, 'Enhanced normalized difference vegetation index (ENDVI)', *Https://Www.Maxmax.Com/Endvi.Htm*, (2015). https://www.maxmax.com/endvi.htm.
42) E. Boegh, H. Soegaard, N. Broge, K. Schelde, A. Thomsen, C.B. Hasager, and N.O. Jensen, 'Airborne multispectral data for quantifying leaf area index, nitrogen concentration, and photosynthetic efficiency in agriculture', *Remote Sensing of Environment*, 81 (*2–3*) 179–193 (2002). doi:10.1016/S0034-4257(01)00342-X.
43) J. Penuelas, F. Baret, and I. Filella, 'Semi-empirical indices to assess carotenoids/chlorophyll a ratio from leaf spectral reflectance', *Photosynthetica*, 31 (*2*) 221–230 (1995).
44) A.A.A. Gitelson, Y.J.J. Kaufman, R. Stark, D. Rundquist, R. Strark, and D. Rundquist, 'Novel algorithms for remote estimation of vegetation fraction', *Remote Sensing of Environment*, 80 (*1*) 76–87 (2002). doi:10.1016/S0034-4257(01)00289-9.
45) J.E. Vogelmann, B.N. Rock, and D.M. Mos, 'Red edge spectral measurements from sugar maple leaves', *International Journal of Remote Sensing*, 14 (*8*) 1563–1575 (1993). doi:10.1080/01431169308953986.
46) J.W. Rouse, R.H. Haas, J.A.S.D.W. Deering, J.A. Schell, D.W. Deering, and J.A.S.D.W. Deering, 'Monitoring vegetation systems in the great plains with ERTS', in: S.C. Becker, Freden E P, Mercanti M A (Eds.), Third Earth Resources Technology Satellite-1 Symposium, NASA. Goddard Space Flight Center 3d ERTS-1, Washington DC, USA, 1974: pp. 309–317.
47) C.J. Tucker, 'Red and photographic infrared linear combinations for monitoring vegetation', *Remote Sensing of Environment*, 8 (*2*) 127–150 (1979). doi:10.1016/0034-4257(79)90013-0.
48) N.W. Darojati, 'Monitoring Drought and Risk of Drought Analysis in Indramayu', Bogor Agriculture University, 2015.
49) D. Ismoyowati, 'To Sustain Sugar Industry in Java, Indonesia: Policies on Sugarcane Supply and The Industry's Performane', Yogyakarta, 2004. doi:10.13140/RG.2.2.34808.85767.
50) G.J. Bellante, S.L. Powell, R.L. Lawrence, R.K. S, and T. Dougher, 'Hyperspectral detection of a subsurface co2 leak in the presence of water-stressed

vegetation', *PLOS ONE*, 9 (*10*) 1–15 (2014). doi:10.1371/journal.pone.0108299.

51) I.D. Sanches, C.R. Souza Filho, L.A. Magalhães, G.C.M. Quitério, M.N. Alves, and W.J. Oliveira, 'Unravelling remote sensing signatures of plants contaminated with gasoline and diesel: an approach using the red edge spectral feature', *Environmental Pollution*, 174 16–27 (2013). doi:10.1016/j.envpol.2012.10.029.
52) T.M. Susantoro, K. Wikantika, D. Sunarjanto, U. Pasarai, B. Widarsono, A. Rahmadi, M. Romli, P. Wahyudi, and S. Kepies, 'CCUS-eor optimization to achieve zero emission program targets in northwest java basin', *EVERGREEN Joint Journal of Novel Carbon Resource Sciences & Green Asia Strategy*, 10 (*03*) 1809–1818 (2023). doi:10.5109/7151730.
53) J.U.H. Eitel, L.A. Vierling, M.E. Litvak, D.S. Long, U. Schulthess, A.A. Ager, D.J. Krofcheck, and L. Stoscheck, 'Broadband, red-edge information from satellites improves early stress detection in a new mexico conifer woodland', *Remote Sensing of Environment*, 115 (*12*) 3640–3646 (2011). doi:10.1016/j.rse.2011.09.002.
54) Y. Hong, F. V.D. Meer, J. Zhang, S.. B. Kroonenberg, F. van der Meer, J. Zhang, and S.. B. Kroonenberg, 'Direct detection of onshore hydrocarbon microseepages by remote sensing techniques', *Remote Sensing Reviews*, 18 (*1*) 1–18 (2000). doi:10.1080/02757250009532381.
55) S. Asadzadeh, and C.R. de Souza Filho, 'Spectral remote sensing for onshore seepage characterization: a critical overview', *Earth-Science Reviews*, 168 48–72 (2017). doi:10.1016/j.earscirev.2017.03.004.
56) Lu Zuhui, Wang Yujin, Chen Dongrong, Li Youming, Xu Aijun, and Yang Fuxing, 'Prospecting oil and gas deposits with cr-39 detectors', *Nuclear Tracks and Radiation Measurements*, 22 (*1*) 387–392 (1993). doi:10.1016/0969-8078(93)90091-H.
57) D.B. Sikka, and R.B. Shives, 'Mechanisms to Explain the Formation of Geochemical Anomalies Over Oilfields. In Near-Surface Hydrocarbon Migration: Mechanisms and Seepage Rates', in: AAPG HEDBERG CONFERENCE, AAPG, Vancouver, Canada, 2001: pp. 1–4.
58) H.M.A. van der Werff, W.H. Bakker, F. van der Meer, and W. Siderius, 'Combining spectral signals and spatial patterns using multiple hough transforms: an application for detection of natural gas seepages', *Computers and Geosciences*, 32 (*9*) 1334–1343 (2006). doi:10.1016/j.cageo.2005.12.003.
59) T.M. Susantoro, H.L. Setiawan, K. Wikantika, A. Saepuloh, and A.H. Harsolumakso, 'An integration of soil spectral and radon measurement for microseepage analysis on onshore hydrocarbon field in indonesia', *International Journal of Tomography and Simulation*, 33 (*2*) 1–13 (2020).
60) H.M.A. van der Werff, M.F. Noomen, M. Van Der Meijde, and F. van der Meer, 'Remote sensing of onshore hydrocarbon seepage: Problems and solutions', in: R.M. Teeuw (Ed.), Mapping Hazardous Terrain Using Remote Sensing, London Geology Society, London, 2007: pp. 125–133. doi:10.1144/SP283.11.
61) D. Schumacher, 'Non-seismic detection of hydrocarbon: an overview', in: AAPG International Conference and Exhibition, The American Association of Petroleum Geologists, Cape Town, South Africa, 2008.
62) T.M. Susantoro, Suliantara, H.L. Setiawan, and K. Wikantika, 'Study of earth surface morphological anomalies based on Landsat OLI 8 data and soil grain size in oil and gas field in undulating morphology', in: The 9th International Seminar on Aerospace Science and Technology (ISAST 2022), Jakarta, Indonesia, 2022: pp. 1–10.
63) M.A. Rasheed, P.L.S. Rao, B. Annapurna, and S.Z. Hasan, 'Implication of soil gas method for prospecting of hydrocarbon microseepage', *International Journal of Petroleum and Petrochemical Engineering*, 1 (*1*) 31–41 (2015).
64) F. van der Meer, P.. Dijk, S.. Kroonenberg, Y. Hong, and H. Lang, 'Hyperspectral Hydrocarbon Microseepage Detection and Monitoring: Potentials and Limitations', in: The 2nd EARSeL Workshop on Imaging Spectroscopy, 11-13 July 2000, ITC, Enschede, The Netherlands., 2000: pp. 1–9.
65) K.G. Osadetz, 'Effects and Impacts of Methane Leakage and Emissions', in: Geoconvention, May 15-19, 2017, Geoconvention, Calgary, Canada, 2017: pp. 1–6.
66) D. Leythaeuser, 'Origin, Migration and Accumulation of Petroleum', in: C. Amadei (Ed.), Encyclopedia of Hydrocarbons, Istituto Della Encyclopedia Italiana, Fondata Da Giovanni Treccani, Roma, 2005: pp. 65–84